

# IMPACT OF LONG DISTANCE PROPAGATED SEISMIC SIGNALS ON THE SOUNDSCAPE IN THE FRAM STRAIT. USE OF ACOBAR DATA AND PE MODELLING.

E Storheim      The Nansen Environmental and Remote Sensing Centre, Bergen, Norway  
A Yamakawa     The Nansen Environmental and Remote Sensing Centre, Bergen, Norway  
H Sagen         The Nansen Environmental and Remote Sensing Centre, Bergen, Norway  
G Pedersen      Christian Michelsen Research AS, Bergen, Norway

## 1 INTRODUCTION

The expected increase in anthropogenic noise in the Arctic, due to increased shipping and resource exploitation, may have a negative influence on the living conditions for marine life. The Fram Strait, and in particular the Marginal Ice Zone (MIZ), is a habitat for marine mammals and fish. It is therefore important to establish a soundscape baseline for this region, and to monitor the changes in the acoustic environment.

One of the key components of anthropogenic sounds is that of seismic airguns, which are used in e.g. seismic surveys for oil and gas exploration, and to map the bathymetric profile and geological properties of the seafloor. These airguns often have a very high source level (SL), which, combined with low attenuation in water for the relevant frequencies, allows for long-range propagation of sound which retains a significant sound pressure level.

Many simulation tools have been developed and used to study the influence of different parameters, such as bathymetry and variability in the ocean environment, on sound propagation<sup>1</sup>. For example, Tronstad & Hovem<sup>2</sup> used ray tracing to investigate propagation of airgun signals over 10 km to 50 km long transects, with range-independent sound speed. The effect of a typical summer and a winter sound speed profile was shown, along with the effect of the bathymetry. Impact on marine life was also discussed. Thode *et al.*<sup>3</sup> investigated airgun signals propagating in the Arctic Ocean, and the influence due to a changing ice cover. In this study, airgun signals were observed from 400 km to 1300 km. Tollefsen and Sagen<sup>4</sup> observed airgun signals originating from the Norwegian Sea 1400 km away, during an experiment with sonobuoys to investigate the spatial variability of ambient noise in the MIZ.

Measurements of the soundscape in the Fram Strait resulted from the ACOBAR<sup>5</sup> ocean acoustic tomography experiment. Seismic airgun activity<sup>6</sup> was observed in a significant amount of the hydrophone recordings made during the experiment. During this study, a seasonal variation in the vertical distribution of the sound was found. The objective of the present work is to analyse this behaviour, and to use simulation tools to illustrate how the sound propagation is affected by: 1) the bathymetry; and 2) the seasonal variability in the sound speed profile between summer and winter.

## 2 METHODS

### 2.1 Experimental configuration

The experimental results presented here are obtained from the ACOBAR<sup>5</sup> (Acoustic Technology for Observing the interior of the Arctic Ocean) acoustic tomography experiment. The project was designed to monitor the properties and transport of water masses to and from the Arctic Ocean through the Fram Strait. It was made up of four distributed vertical line arrays (DVLA), placed in the Fram Strait between Svalbard and Greenland, illustrated by the large black and red triangles in Figure 1.

Recordings from mooring D are used in the present work. 8 hydrophones were distributed along the vertical mooring at design depths of 227.9 m, 323.9 m, 419.9 m, 515.9 m, 614.2 m, 710.2 m, 806.2 m, and 902.2 m. The sampling frequency is 1000 Hz, and recordings were made between 10 Hz and 500 Hz for 100 seconds, every third hour over two years. The measurement results shown in Section 3.2 are obtained from mooring D at two different dates: 1) 2011-02-22; and 2) 2011-07-19.

## 2.2 Simulation setup

The 2D simulations of the transmission loss (TL) as a function of range,  $r$ , and depth,  $z$ , are performed using RAM<sup>7</sup>. A point source with unit amplitude and a 100 Hz frequency is placed at 10 m depth. The source radiates into lossless water with a flat water/vacuum interface at the top, and a semi-infinite, range-dependent bottom profile. The simulation results are shown in terms of the signal level  $S$ , given by the passive sonar equation as<sup>1</sup>

$$S = SL - TL, \quad (1)$$

where  $SL$  is the source level. The source level used here is 250 dB re 1  $\mu$ Pa. The absorption in seawater is assumed to be negligible for the frequencies used here.

The range-dependent sound speed profile is obtained from the 2013 World Ocean Atlas<sup>8</sup> (WOA13), with a  $1/4^\circ$  resolution. The bathymetric profile is obtained from the International Bathymetric Chart of the Arctic Ocean<sup>9</sup> (IBCAO). The material properties used for the bottom are: a longitudinal sound speed of 3000 m/s, a density of 1500 kg/m<sup>3</sup>, and an attenuation of longitudinal waves of 1.5 dB/ $\lambda$ . These parameters are for the present case set to range-independent.

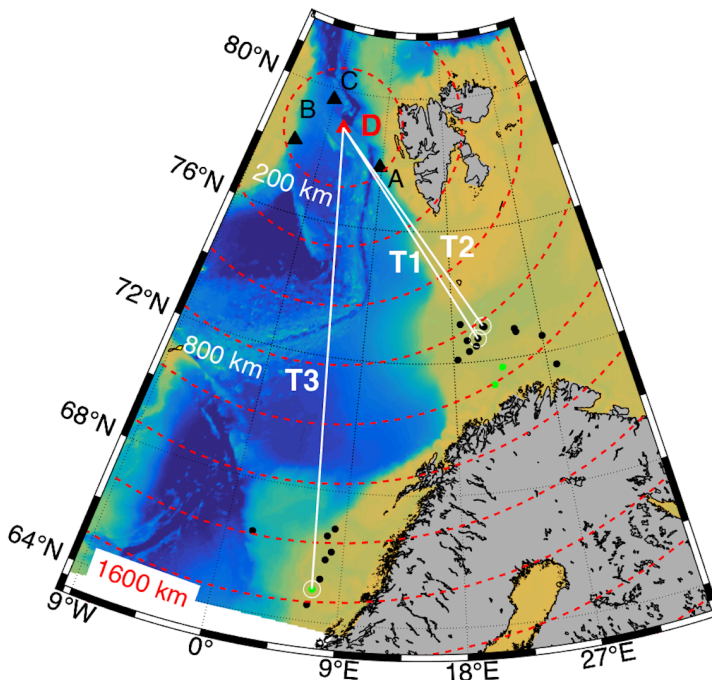
Three different transects are investigated in the following, from two regions: Two from the Barents Sea, denoted T1, and T2; and T3 in the Norwegian Sea, cf. Figure 1. These are selected based on the bathymetric conditions and the spatial variation in the sound speed profiles. The simulations are performed with a uniform spatial resolution of  $\Delta r = 500$  m in the horizontal direction, while the vertical resolution is depth-dependent. The profile is sampled every 5 m above 100 m, every 25 m from 100 m until 500 m, every 50 m from 500 m to 1000 m, and every 100 m below 1000 m.

## 3 RESULTS

### 3.1 Seismic surveys

General information about seismic surveys in Norwegian territorial waters, such as the time period, region, and the size and number of airguns used, is available from the Norwegian Petroleum Directorate (NPD)<sup>10</sup>. Typically, most of the activity is performed in the summer time, due to e.g. poor weather or low-light conditions in the winter. For the present case, 6 different surveys were performed in the winter period, and 33 different surveys in the summer period. The activity occurs in three main regions (north to south): The Barents Sea; the Norwegian Sea; and the North Sea. Figure 1 shows the distribution of seismic surveys off the coast of Norway. The closest survey is in the Barents Sea approximately 770 km from mooring D, while the furthest survey is in the North Sea, approximately 2500 km away.

**Figure 1:** Overview of the seismic survey locations from 12<sup>th</sup> to 19<sup>th</sup> July 2011 (black dots), and 21<sup>st</sup> to 28<sup>th</sup> February 2011 (green dots). The red dashed circular lines indicate 200 km intervals from the mooring D (red triangle). The white lines marks the paths between the sources and receiver positions used in the simulations, T1-T3. The remaining moorings in the ACOBAR project is illustrated by the black triangles.



The NPD does not provide the position of seismic vessels as a function of time, or information about the time when the airguns are actually in use. However, this may be estimated from the Automatic Identification System (AIS), based on the behaviour and track of the vessels.

This information, obtained from the Norwegian Coastal Administration<sup>11</sup> (NCA), is used in the present work to investigate the likely origins of the signals observed in the hydrophone recordings.

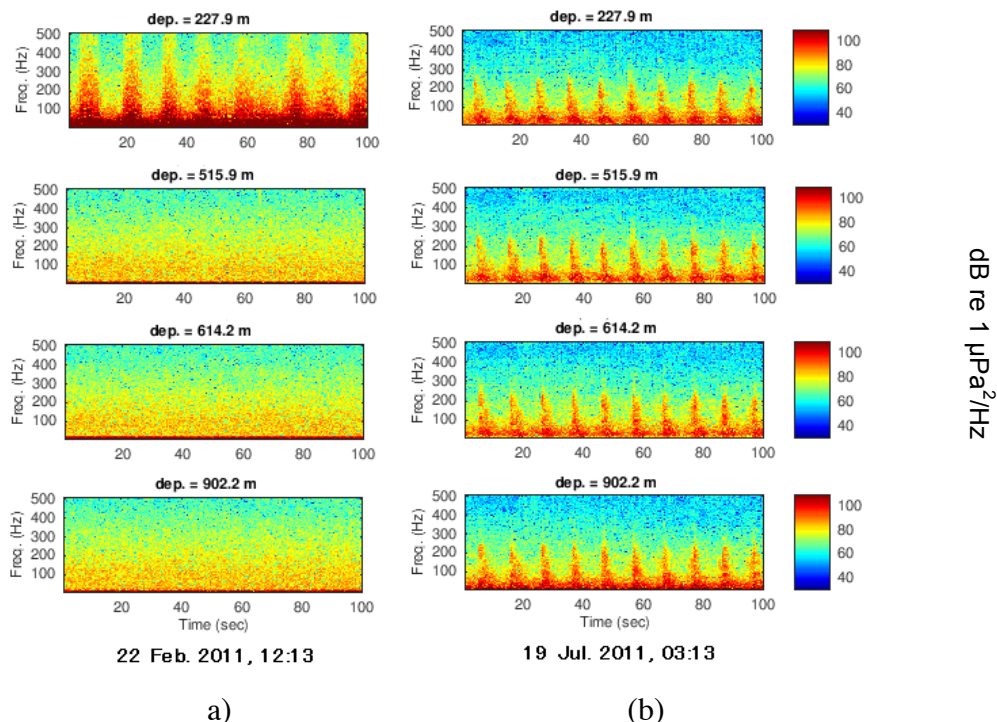
### 3.2 Hydrophone recordings

Figure 2 shows frequency spectra of the recordings made at four of the hydrophones on the 22<sup>nd</sup> of February 2011 (a), and on the 19<sup>th</sup> on July 2011 (b). These spectrograms illustrate the typical behaviour found throughout the experiment: In the winter, seismic signals are in most cases only observed at the upper hydrophone, while the signals are observed on all the hydrophones in the summer.

In (a) the seismic signals are only observed at the upper most hydrophone. The time interval between shots is approximately 13 seconds, and spans the entire 500 Hz frequency band. This distribution indicates that a surface channel may be present, which allows for the long-range propagation of sound. However, the seismic survey activity is low in the wintertime due to e.g. bad weather and extent of sea ice. Analysis of AIS data shows that only one ship is performing seismic surveys at this time, located in the Norwegian Sea approximately 1560 km from the receiver. This position is marked by the T3 track. However, ships operating in other countries may also be doing surveys at the same time.

The upper hydrophone is located near the lower part of the surface channel when the entire array is vertical. However, ocean currents induce a mooring motion that increases the depth of the hydrophones, thereby moving the upper hydrophone below the surface duct. Sometimes in the winter, the seismic signals found on the upper hydrophone would suddenly disappear. This may be caused by e.g. this motion of the mooring, or by pauses in the surveys. The variability in the sound speed will also have a great influence on the propagation.

In the summer (b) the signal is observed at each of the four hydrophones shown here, and appears to be uniformly distributed along the array. The signals are not as strong compared to those in (a) and are only seen below 250 Hz. The same characteristic time interval between shots is also seen, but with a higher shot frequency. The time between each shot is approximately 10 s. These signals are most like originating from the Barents Sea, but no specific survey could be identified.



**Figure 2:** Frequency spectra of the recordings made on 2011-02-22 (a) and 2011-07-19 (b) for four of the receiver hydrophones.

### 3.3 Simulation results

#### 3.3.1 Source placed in the Barents Sea

Figures 3 and 4 shows the sound speed map from WOA13 as a function of range and depth for the winter and summer profiles, and the corresponding signal levels calculated with RAM, for transect T1 and T2 originating in the Barents Sea.

The winter sound speed profile along T1 shown in Figure 3(a) has a warm part near the source until 100 km, a cooler part between 100 and 300 km, and after that there is a warm region. A cold front that extends down to 1100 m is present from 600 km until the receiver at 845 km. The source is located on the Barents shelf where the depth is 480 m. The bathymetry is fairly flat until 100 km, where the depth decreases to approximately 150 m. The depth increases to 400 m at 280 km, and after that the depth increases gradually to 2000 m at 500 m. The depth increases gradually to 2450 m at the receiver, with a 3500 m deep canyon present near 670 km range.

The summer sound speed profile (b) has a similar structure as the winter profile until 300 km range. Beyond 300 km there is a warm part close to the surface, which extends down to 800 m depth. This warm surface layer is reduced in extent as the range increases, i.e. the surface gradient becomes less steep.

The sound propagates in (c) in a surface duct, and in a downward-refracted part after 400 km when the depth increases. This is refracted upwards towards the receiver range, where the sound is distributed between 0 and 1300 m depth. The duct extends down to 170 m depth from 600 km to the receiver range.

With the summer profile the sound is seen to only propagate in a duct below the surface, approximately 600 m-800 m in extent. Downsloping<sup>3</sup> occurs at 400 km when the depth increases,

after which the sound is slowly refracted upwards as the range increases. At the receiver range the sound is distributed between 200 m and 1000 m depth.

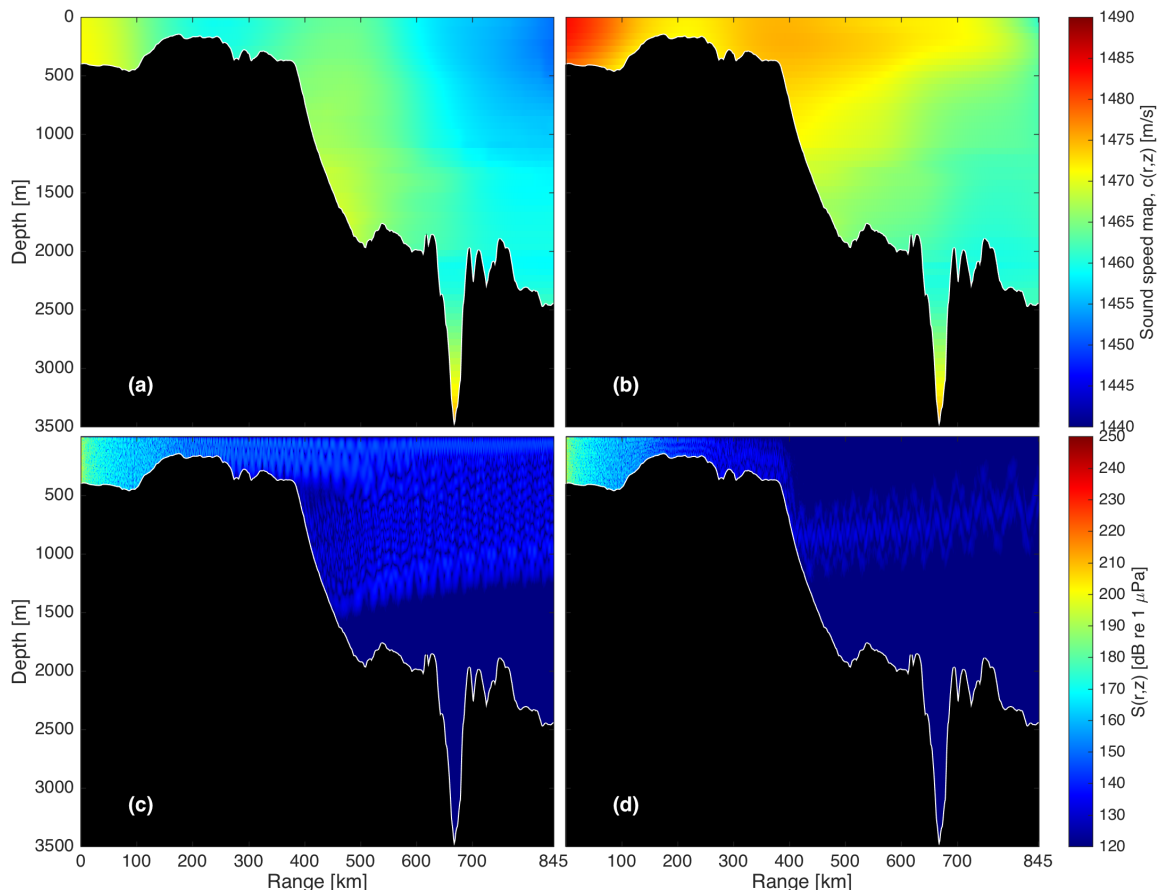


**Figure 3:** Sound speed profile (upper row) from WOA13 for transect T1, and corresponding source level plot (lower row) calculated with RAM, for the winter profile (left column) and the summer profile (right column).

The SSP along T2 is very similar to T1 since the two source positions are very close together, i.e. approximately 50 km apart, both for the winter and summer profiles, cf. Figure 4(a) and (b). The bathymetry is also very similar for the two transects, and the significant difference is the depth along the most shallow part from 150 km to 300 km range: For T1 the most shallow part is at 154 m, while for T2 the minimum depth is 42 m.

Along transect T2 with the winter profile, the sound only propagates in the surface duct after the shallow part near 200 km range; no downward refraction occurs. The duct extends down to approximately 200 m depth. With the summer profile (b) the sound is trapped within the shallow part, out to 150 km range, since there is no surface duct present.

There is a similar behavior for the sound propagation as observed for T1, i.e. downsloping occurs near 200 km, and sound propagates within a channel below the surface which is refracted upwards towards the receiver range.

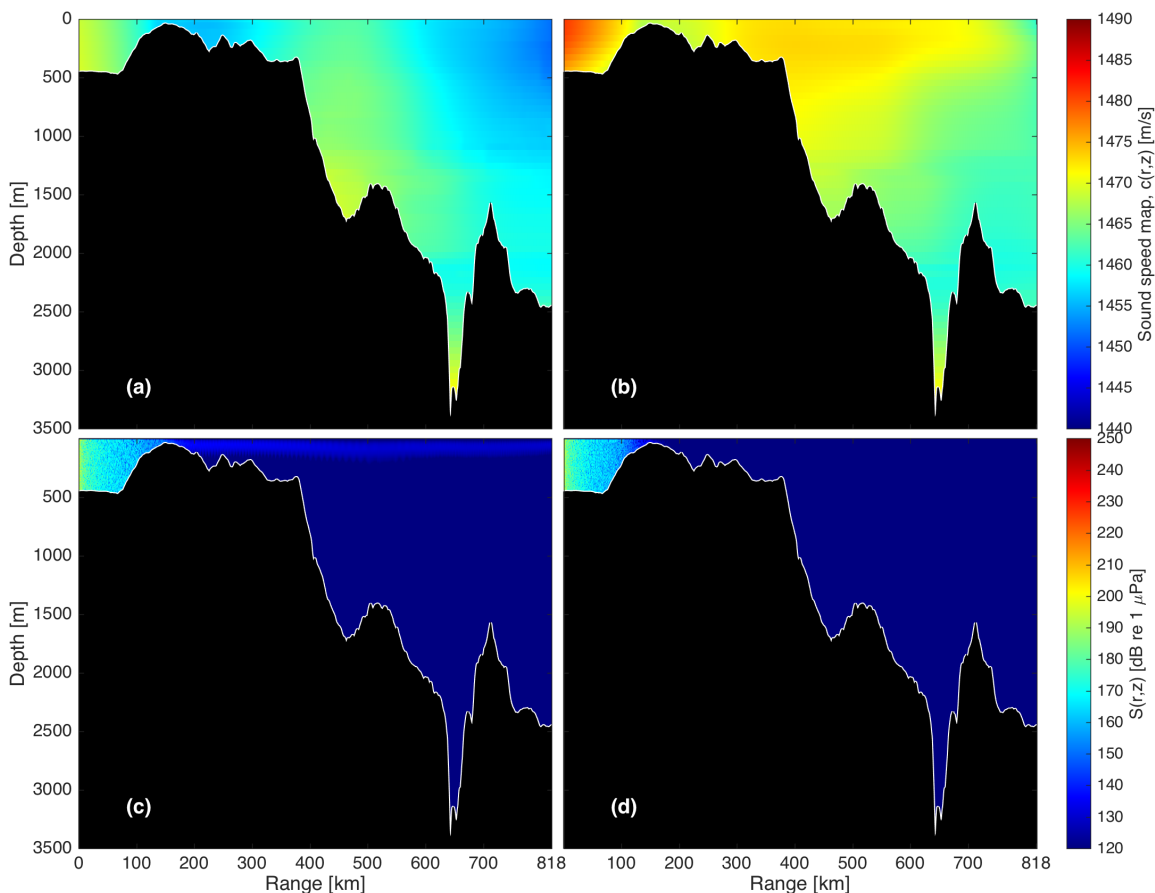


**Figure 4:** Sound speed profile (upper row) from WOA13 for transect T2, and corresponding source level plot (lower row) calculated with RAM, for the winter profile (left column) and the summer profile (right column).

### 3.3.2 Source placed in the Norwegian Sea

Figure 5 shows the sound speed map from WOA13 as a function of range and depth for the winter and summer profiles, and the corresponding signal level calculated with RAM, for transect T3 originating from the Norwegian Sea.

For the winter profile (a) there is a very distinct difference between the behavior prior and after 900 km, with a warm part to the left and a cold part to the right, where both extend down to 2100 m depth. A similar difference in characteristics at 900 km is also observed for the summer profile (b), but in this case the vertical variation is more significant compared to the winter profile.

Compared to T1 and T2 for a source in the Barents Sea, the bathymetry is qualitatively similar, with the source located on a shelf 300 m-500 m deep, radiating towards a deeper part ~3000 m. The most significant difference is that the really shallow part (~100 m depth) on the shelf is not present for T3.

For signal level plot using the winter profile (c) along T3 the sound is seen to fill the entire water column. A very distinct channel below the surface is observed after 180 km range, where the signal level is the highest. This behavior is very similar to that observed for T1, cf. Figure 3(c), except that there is a very distinct upward refraction near 800 km, where the channel extends to the surface. The overall behavior for the winter (c) and summer profile (d) is very similar, except that there is less sound near the surface between 300 km and 800 km.

Transect T3 with the winter profile corresponds to the case observed in the measurements, cf. Figure 2(b). However, for the simulation result the sound is distributed throughout the water column, not only near the surface, as observed in the measurements.

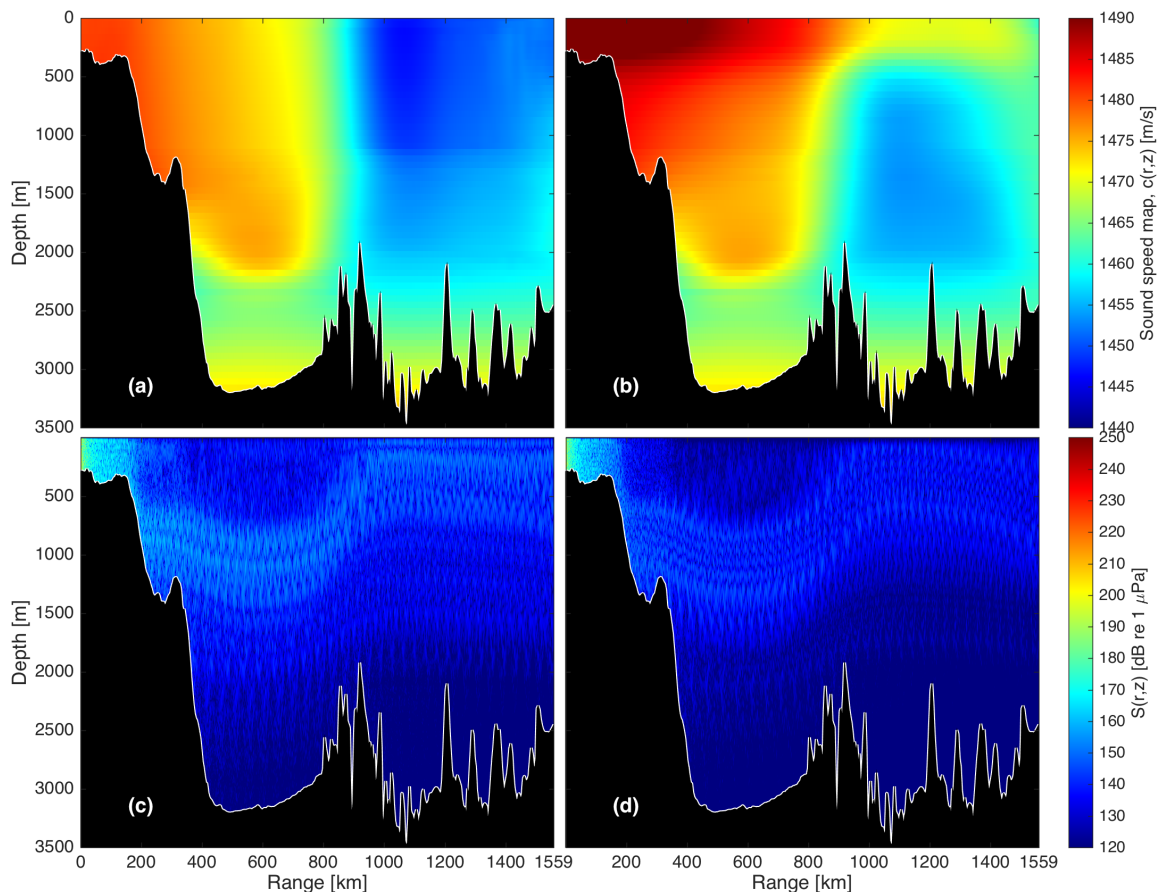


**Figure 5:** Sound speed profile (upper row) from WOA13 for transect T3, and corresponding signal level plot (lower row) calculated with RAM, for the winter profile (left column) and the summer profile (right column).

## 4 SUMMARY AND CONCLUSIONS

Analysis of measurements from the ACOBAR experiment shows that the depth-dependence observed for seismic airgun signals in the acoustic recordings is different during summer and winter. In the winter, the seismic airgun signals are often only observed at the upper hydrophone close to the surface, while the signals are present at all the hydrophones during the summer. Modelling tools are used to show how seasonal variation in the sound speed profile, along with bathymetric effects may explain this behaviour.

A simplified seasonal environmental input has been used with RAM to study the sound propagation from selected points in the Barents Sea and the Norwegian Sea towards the Fram Strait, respectively, to illustrate how seismic airgun signals may propagate. The seismic source is modelled as a 100 Hz monochromatic point source. The seasonal variability in the oceanographic fields is taken from the World Ocean Atlas. The bathymetric profile was obtained from IBCAO. No range-dependency in the geo-acoustic information was included. Using this simple approach, the same vertical distribution observed in the measurements is reproduced, to some extent. There is

however a difference of approximately 50 dB between measurements and simulations at 100 Hz, where the simulations overestimate the signal level for a 250 dB re 1  $\mu$ Pa source.

For the two sources located in the Barents Sea, simulations show that the bathymetry has a significant influence on the amount of acoustic energy that enters the deep water. In the deeper water areas, the oceanographic conditions determine the distribution of the sound in the water column. This is particularly seen for the winter profile, where the presence of a surface duct allows for sound propagation over the shallow part.

For the source located in the Norwegian Sea, the acoustic propagation is less influenced by the bathymetry. The signal level is higher in the winter than in the summer, and a distinct sound channel is observed. Significant refraction does also occur when the sound encounters the cold front.

## 5 ACKNOWLEDGEMENT

The present work has been financed by the UNDER-ICE project. Data is obtained from the EU project ACOBAR.

## 6 REFERENCES

1. Jensen, F.B. *et al.*, *Computational Ocean Acoustics*, 2nd ed., New York: Springer (2011).
2. Tronstad T.V. and Hovem J.M., "Bathymetric and seasonal effects on the propagation of airgun signals to long distances in the ocean", in *Proceedings of the OCEANS 2011 Conference, 19-22 Sept. 2011, Waikoloa, USA* (2011)
3. Thode, A. *et al.*, "Long range transmission loss of broadband seismic pulses in the Arctic under ice-free conditions", *J. Acoust. Soc. Am.*, **128**, pp.EL181-L187 (2010).
4. Tollefsen, D. & Sagen, H., "Seismic exploration noise reduction in the Marginal Ice Zone", *J. Acoust. Soc. Am.*, **136**(1), pp.EL47-EL52 (2014).
5. ACOBAR - Acoustic Technology for Observing the Interior of the Arctic Ocean. Available online (last checked: 2016-10-26): <https://acobar.nersc.no>
6. Yamakawa, A. *et al.*, "Soundscape characterization and the impact of environmental factors in the central part of the Fram Strait", in *Proceedings of the 2016 Acoustic and Environmental Variability, Fluctuations and Coherence Conference, 12-13 December 2016, Cambridge, UK* (2016).
7. Collins, M.D., "A split-step Padé solution for the parabolic equation method", *J. Acoust. Soc. Am.*, **93**(4), pp.1736–1742 (1993).
8. Boyer, T.P. *et al.*, "World Ocean Database 2013, NOAA Atlas NESDIS 72", S. Levitus (Ed.), A. Mishonov (Technical Ed.); Silver Spring, MD (2013).
9. Jakobsson, M. *et al.*, "The International Bathymetric Chart of the Arctic Ocean (IBCAO) Version 3.0", *Geophysical Research Letters*, **39**(12), pp.1–6 (2012).
10. The Norwegian Petroleum Directorate – Seismic. Available online (last checked: 2016-10-24) <http://www.npd.no/en/Seismic/>
11. The Norwegian Coastal Administration – AIS. Available online (last checked: 2016-10-24): <http://www.kystverket.no/Maritime-tjenester/Meldings--og-informasjontjenester/AIS/AIS-Norge/>